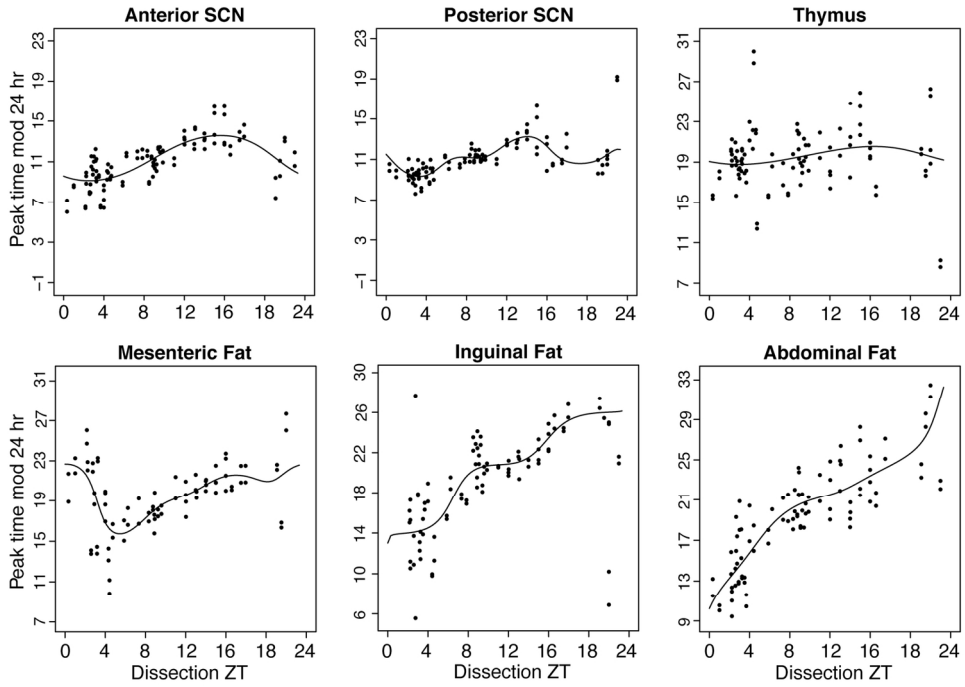

Supplementary Figure S1. Mice from control T24 LD cycles showed phase of bioluminescence rhythms measured ex vivo that varied with time of dissection. Data for different tissues is shown in separate graphs and each mouse contributes at most two points per graph (1st and 2nd peak times mod 24, excluding samples which failed rhythmicity criterion). Solid black lines show the circular-circular regression for each tissue, reflecting its resetting curve. Time of dissection is calculated relative to the LD cycle, with ZT0 set to the time of lights on. Peak time of each explant was calculated by the procedure described in the text and plotted on a modulo-24 h scale.

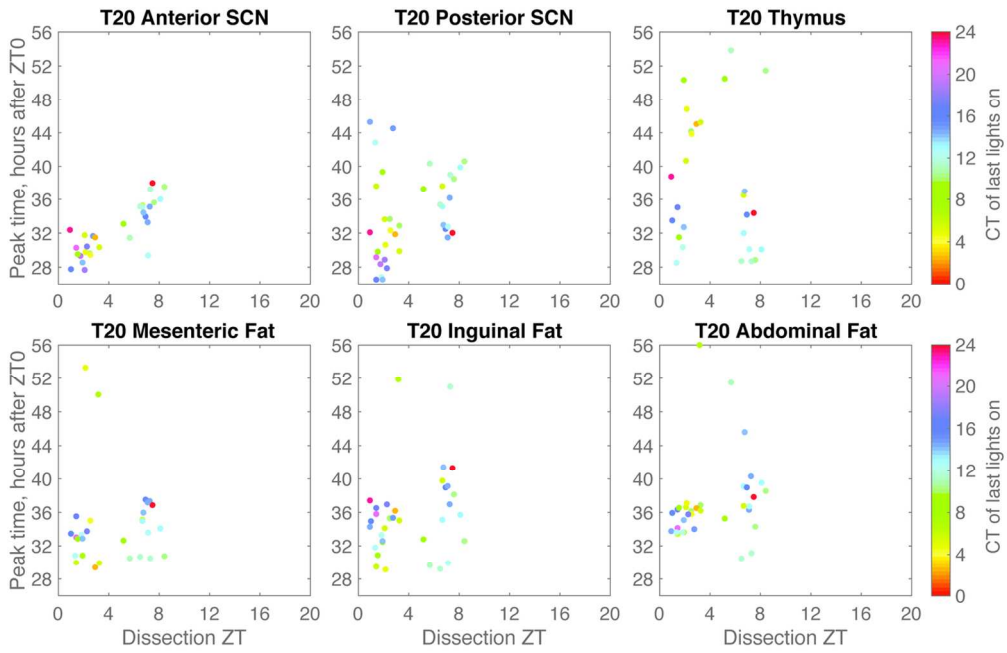

Supplementary Figure S2. Mice from T20 LD cycles showed phase of bioluminescence rhythms measured ex vivo that varied with time of dissection. Data for different tissues is shown in separate graphs and each mouse contributes at most one point per graph (we excluded samples which failed rhythmicity criterion). Time of dissection is calculated relative to the LD cycle, with ZT0 set to the last time of lights on before dissection. Color indicates the estimated CT at last lights on: red indicates that CT and ZT are well-aligned, while light blue indicates CT and ZT are maximally misaligned. Because these mice did not entrain to T20, CT changes its relative alignment with ZT each day, making CT at last lights on a further variable in addition to time of dissection. Anterior SCN shows strong resetting of phase with respect to dissection time, while posterior SCN exhibits a more spread out set of phases. A possible explanation for this difference is that the last lights on acted as a phase-delaying light pulse for some of the animals for which last lights on coincided with CT 9-16 (green to dark blue). The posterior SCN points well off the diagonal may have been less susceptible to strong resetting by dissection due to containing more clock neurons than other slices. Note that estimated CT at last lights on is based on body temperature rhythm phase preceding last lights on, so doesn't take into account potential phase-shifting effects of that last light exposure. The thymus shows no pattern with respect to ZT because its phase aligns with CT, as shown in Figure 6. The phases show variability, with a trend that is consistent with strong resetting of phase by dissection, as indicated in Figure 6 when plotted with respect to CT.

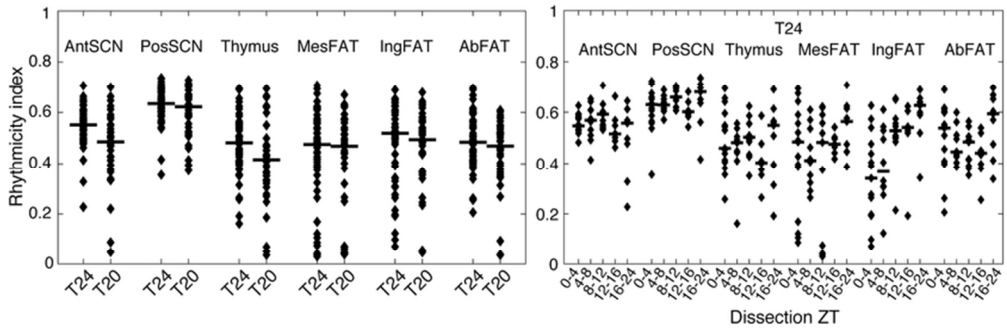

Supplementary Figure S3. Left: Comparison of the rhythmicity index (RI) for PER2::LUC bioluminescent rhythms of tissues sampled from mice housed in either T24 or T20. Right: Comparison of RI across dissection times for T24 condition.

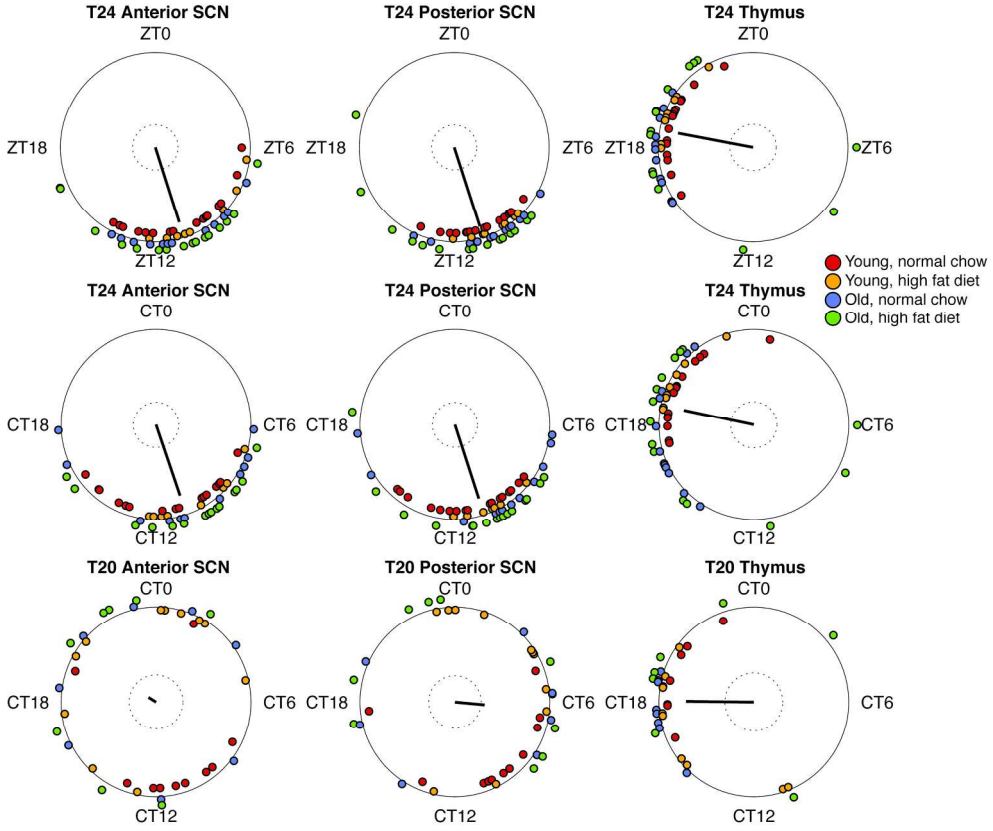

Supplementary Figure S4. Circular plots of peak time relative to extrapolated ZT (1st row) or CT (2nd and 3rd rows) of PER2:LUC bioluminescent rhythms of select tissues in mice from T24 or T20 lighting cycles. Results are color coded according to diet and age conditions.

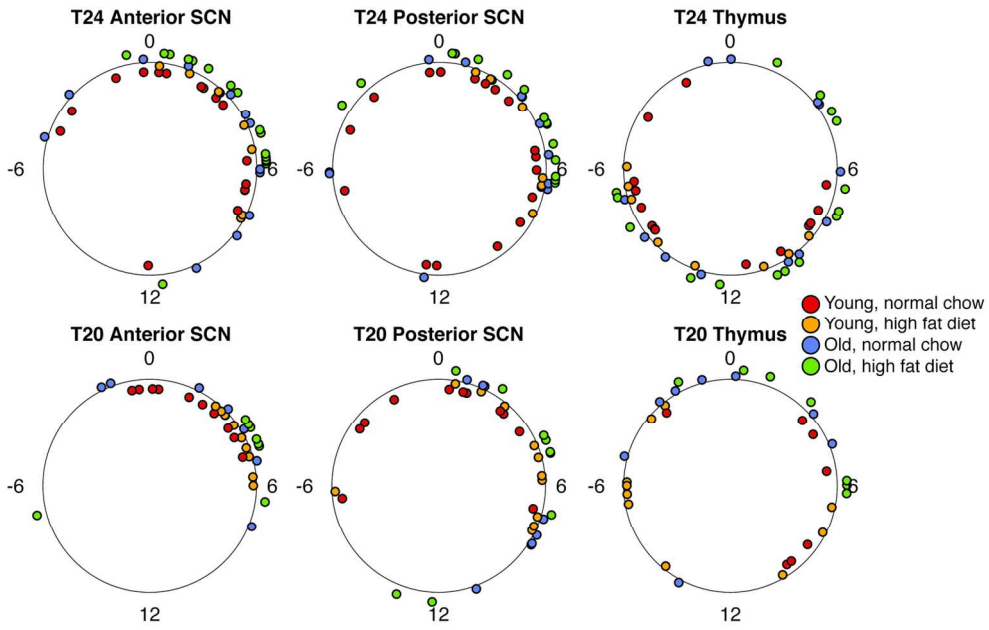

Supplementary Figure S5. Circular plots of peak time relative to dissection time of PER2:LUC bioluminescent rhythms of select tissues in mice from T24 or T20 lighting cycles. Results are color coded according to diet and age conditions. Time is hours after dissection mod 24.

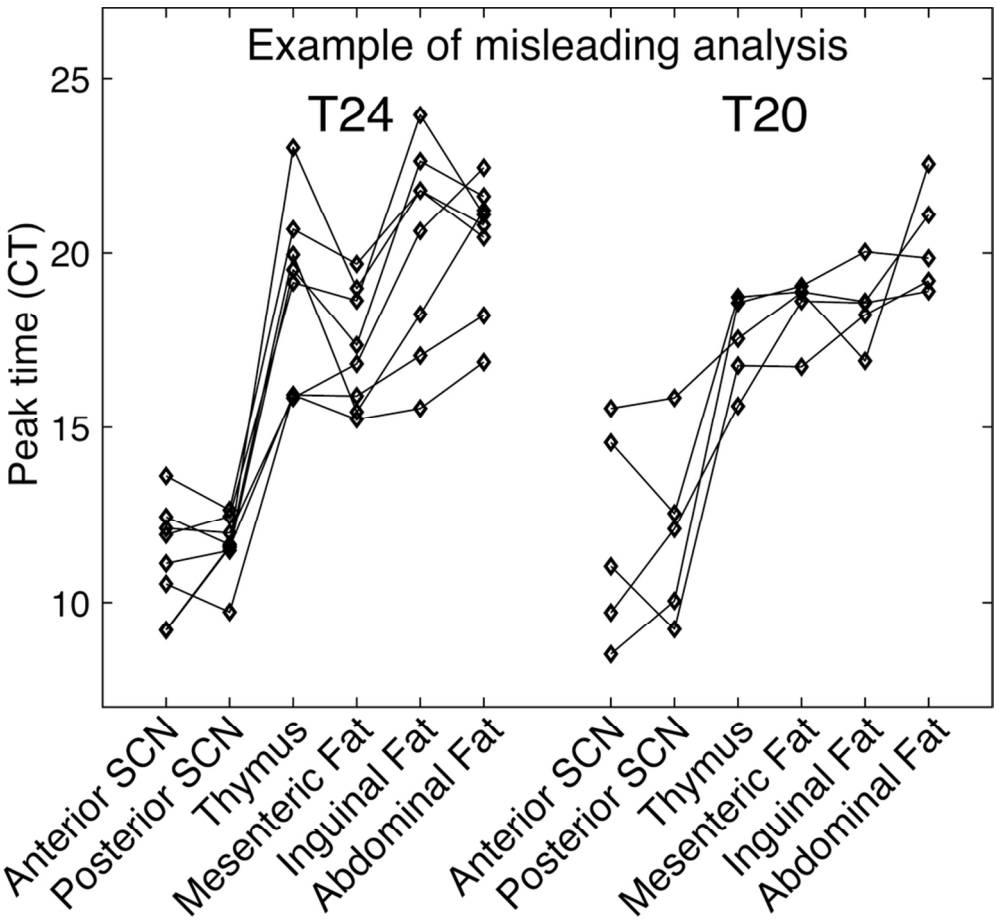

Supplementary Figure S6. Phase results for animals in the current experiment, restricted to just those animals dissected during ZT6-12. This graph illustrates that results from such a hypothetical experiment, where we controlled time of dissection, would have produced results that look reasonably consistent and interpretable, yet are misleading. In particular, fat tissues phases are strongly reset under both T24 and T20, and SCN phases are reset under T20, so the phases indicated in this figure are not valid.